Molecular Crystals and Liquid Crystals
Publication details, including instructions for authors and subscription information:
http://www.tandfonline.com/loi/gmcl20

Influence of Moieties and Chain Length on the Abundance of Orthogonal and Tilted Phases of Linear Hydrogen-Bonded Liquid Crystals, Py16BA:nOBAs

Sangeetha G. Bhat [a], M. Srinivasulu [a], S. R. Girish [a], Padmalatha [a], Poornima Bhagavath [a], S. Mahabaleshwara [a], D. M. Potukuchi [b] & M. Muniprasad [b]

[a] Department of Chemistry, Manipal Institute of Technology, Manipal University, Manipal, India

[b] Department of Physics, University College of Engineering, Jawaharlal Nehru Technological University, Kakinada, India

Available online: 27 Dec 2011

To cite this article: Sangeetha G. Bhat, M. Srinivasulu, S. R. Girish, Padmalatha, Poornima Bhagavath, S. Mahabaleshwara, D. M. Potukuchi & M. Muniprasad (2012): Influence of Moieties and Chain Length on the Abundance of Orthogonal and Tilted Phases of Linear Hydrogen-Bonded Liquid Crystals, Py16BA:nOBAs, Molecular Crystals and Liquid Crystals, 552:1, 83-96

To link to this article: http://dx.doi.org/10.1080/15421406.2011.604569

Mol. Cryst. Liq. Cryst., Vol. 552: pp. 83–96, 2012

ISSN: 1542-1406 print/1563-5287 online
DOI: 10.1080/15421406.2011.604569

Taylor & Francis
Taylor & Francis Group

Influence of Moieties and Chain Length on the Abundance of Orthogonal and Tilted Phases of Linear Hydrogen-Bonded Liquid Crystals, Py16BA:nOBAs

SANGEETHA G. BHAT,[1] M. SRINIVASULU,[1] S. R. GIRISH,[1] PADMALATHA,[1] POORNIMA BHAGAVATH,[1] S. MAHABALESHWARA,[1] D. M. POTUKUCHI,[2,*] AND M. MUNIPRASAD[2]

[1]Department of Chemistry, Manipal Institute of Technology, Manipal University, Manipal, India
[2]Department of Physics, University College of Engineering, Jawaharlal Nehru Technological University, Kakinada, India

A novel series of linear hydrogen-bonded (HB) liquid crystalline (LC) complexes (HBLCs), namely Py16BA:noBAs, is reported. The series was prepared by the complexation of a novel non-mesogenic proton acceptor moiety, namely (4-pyridyl)-benzylidene-4′-n-hexadecyl aniline (Py16BA), with a mesogenic proton donor, p-n-alkoxy benzoic acid (noBAs for n = 3, 4, 5, 6, 7, 8, 9, and 12) moieties. Formation of HB complexes is confirmed through FTIR spectra. The LC phases exhibited by Py16BA:noBAs, the transition temperatures (T_c), and the heat of transition (enthalpy) (ΔH) are determined by polarizing optical microscope (POM) and differential scanning calorimetry (DSC) techniques. A comparative study of phase abundance is presented (with respect to the HB complexes of pure noBAs). An orthogonal smectic-A phase is induced by quenching the nematic phase in the lower homologs, while a quasi-2D tilted smectic-F phase is induced in the intermediate (or higher) homologs Py16BA:noBAs. The odd–even effect is observed across the isotropic–LC phase and LC–solid phase transitions. Overall mesogenic stability is enhanced. Optimization of the tilted smectic phase stability is discussed in the wake of the configuration of hydrogen bonding and the steric intrusion due to the increase in length of the flexible end-chain. Based on the extrapolation of the odd–even effect, an ACBF multi-critical point is predicted in the phase diagram in the vicinity of intermediate homologs, possibly in a binary of Py16BA:5oBA and Py16BA:6oBA.

Keywords Hydrogen bonded liquid crystal, pyridyl derivative, re-entrant SmC, tilt angle, order parameter fluctuations

*Address correspondence to D. M. Potukuchi, Department of Physics, University College of Engineering, Jawaharlal Nehru Technological University, Kakinada 533 003, India. E-mail: potukuchidm@yahoo.com

1. Introduction

The application of noncovalent interaction involved with the design of functional organic materials is a widely discussed topic [1]. Hydrogen bonding has been emerging as a powerful tool for assembling molecules and building supra-molecular structures due to its stability and directionality [2]. Liquid crystalline (LC) materials are known to possess anisotropic properties and are recognized as new dynamic functional materials [3]. Although the relevance of hydrogen bonding in supra-molecular LCs were reported in the 1960s [4,5], optimization and tailoring of their utility in electro-optic devices is an emerging topic of the last two decades only [6–12]. Further, hydrogen bonding is known to influence the thermal stability and its response to external fields in the phases of device interest [13–16]. As such, the presence of hydrogen bonding in LC materials needs to be investigated with regard to the realization of LC phases (of device interest), their stability, and their response to the stimulus. In continuation of our ongoing research activity in HBLCs (involving linear, double, alternative, and complementary types of hydrogen bonding) regarding the study of influence of moieties in realizing LC phases of device interest [9,10,16,17], a new series of HBLCs involving hydrogen bond between a pyridyl derivative of long chain p-n-alkylaniline (the N atom in it enacts as a proton acceptor moiety) and a p-n-alkoxy carboxylic acid (the H atom in the $-$COOH group acts as a proton donor moiety) is prepared.

2. Experimental

2.1 Materials and Methods

The chemical ingredients, namely 4-pyridine carboxaldehyde, 4-hexadecyl aniline, and 4-n-alkoxy benzoic acids, in their pure form are procured from Aldrich, USA. Double-distilled ethanol, acetic acid, and tetrahydrofuran (THF) are procured from CDH, India. The IR spectra of the products are recorded using Shimadzu-8701 FTIR spectrophotometer. The LC phases are characterized by their textures using SDTECH's (India) polarizing optical microscope (POM) (with crossed polars) in conjunction with a hot stage. The heating and cooling rates employed for textural observations are 5°C/min. The accuracy of the temperature measurements is ± 0.1°C. The transition temperatures T_c and the enthalpy ΔH associated with LC phase transitions are determined by Shimadzu DSC-60. The heating and cooling rates employed in calorimetry are 5°C/min.

2.2 Preparation of (4-Pyridyl)-Benzylidene-4′-n-Hexadecyl Aniline (Py16BA)

The Py16BA is prepared as per the reported procedure [18]. To 1.07 g (0.1 mmol) of 4-pyridine carboxaldehyde in absolute ethanol, 3.17 g (0.1 mmol) of 4-hexadecyl aniline in ethanol and 3–4 drops of glacial acetic acid as a catalyst is added and refluxed for 3 h. After refluxing the reactants, the volume of the solvent is reduced to half by distillation. The resulting solution is kept in an ice bath for few minutes. A white shiny crystalline powder is obtained. This is re-crystallized with hot ethanol several times. The yield is about 78%. The melting point for this product is found to be around 68°C. The synthetic route for the preparation is shown in Scheme 1.

2.3 Preparation of HBLC Complexes

The HBLC complexes, namely Py16BA**:**noBAs, are prepared by the following standard procedure [19] (Scheme 2). 4-Alkoxy benzoic acids (i.e., for propyl-to-nonyl and

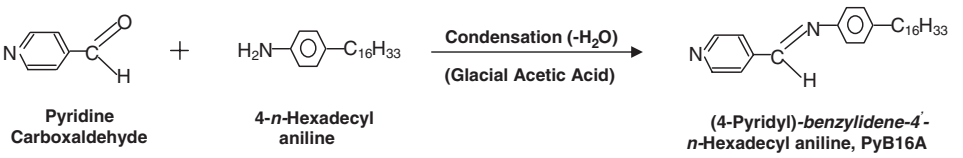

Scheme 1. Synthetic route for the preparation of Py16BA.

dodecyl analogs of noBAs) are added to excess anhydrous THF solution. Thus, the naturally existing dimeric form with complementary hydrogen bonding in noBAs is converted into the monomeric form. To 1.015 g (2.5 mmol) of (4-pyridyl)-benzylidene-4′-n-hexadecyl aniline (in anhydrous THF solution), an equivalent amount of (2.5 mmol) noBAs (where $n = 3$–9 and 12) is added (in the presence of excess anhydrous THF solution). The mixture is refluxed for 3 h and then stirred overnight at room temperature. After removing the solvent by distillation, the HBLC complexes are isolated. The general name proposed for the present HBLCs is Py16BA**:**noBA, while its molecular formula is depicted in Scheme 2.

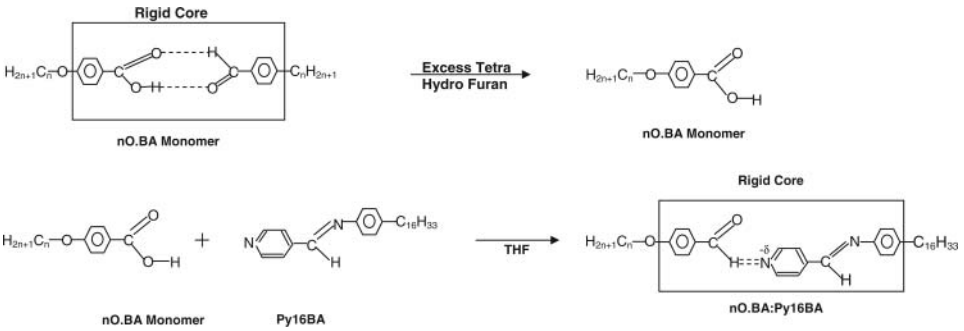

Scheme 2. Molecular structure of Py16BA:noBA complexes.

3. Results and Discussion

3.1 Confirmation of Hydrogen Bonding by FTIR Studies

The details of observed FTIR peaks (in cm^{-1}) along with the underlying functional groups as exhibited by the present HBLC complexes, Py16BA:noBAs series, are presented in Table 1.

The proton acceptor moiety, namely (4-pyridyl)-benzylidene-4′-n-hexadecyl aniline (Py16BA), is characterized by solid-state (KBr) FTIR spectroscopy. The FTIR spectrum of PyB16A is presented in Fig. 1. In the FTIR spectra, any peak above 3000 cm^{-1}, expected to be of $-NH_2$ group of hexadecyl aniline, is found to be missing, which implies the absence of the p-n-hexadecyl aniline product [20]. The observed absence of peaks in the range of 1715–1695 cm^{-1}, characteristic of carbonyl stretching (i.e., C=O of pyridylbenzaldehyde), implies the absence of the aldehyde group in Py16BA. Furthermore, the observed peak at 2996 cm^{-1} implies that the C−H stretching of pyridine is maintained, intact with its aromatic ring. The doublet absorption line observed at 2918 cm^{-1} and 2847 cm^{-1} implies the C−H stretching of aldehyde due to Fermi resonance. The observed peak at 1625 cm^{-1}

Table 1. Data of IR absorption (in cm^{-1}) observed for the HBLC complexes (Py16BA:noBAs)

HBLC complex	υ_{C-H} aromatic (cm^{-1})	υ_{OH} (cm^{-1})	$\upsilon_{C=O}$ (cm^{-1})	$\upsilon_{C=N}$ of pyridine (cm^{-1})
Py16BA:3oBA	3030	2964	1681	1608
Py16BA:4oBA	3037	2964	1693	1608
Py16BA:6oBA	3037	2964	1687	1603
Py16BA:7oBA	3037	2958	1693	1597
Py16BA:8oBA	3037	2958	1687	1603
Py16BA:9oBA	3037	2952	1687	1603
Py16BA:12oBA	3036	2964	1705	1614

implies the C=N stretching of the Schiff's base. The observed peak at 1596 cm^{-1} implies the C=N stretching of the pyridine moiety. The observed double peak at 825 cm^{-1} and 815 cm^{-1} implies the out-of-plane bending of C—H corresponding to the 4-substituted pyridine moiety. Thus, the appearance of a double peak confirms the formation of an imine group in the Py16BA moiety. The N-atom in the imine group of pyridylbenzaldehyde may be considered as a proton acceptor in the ongoing hydrogen bonding with a possible proton donor moiety.

The H-atom in the acid group of noBA (4-n-alkoxy benzoic acids) represents the proton donor during the formation of hydrogen bonding. Solid-state (KBr) FTIR spectrum of the 4-n-pentyloxy benzoic acid (5oBA) is presented in Fig. 2 as a representation. The noBAs are known to exist as dimers at room temperature [21]. The spectrum shows a very broad

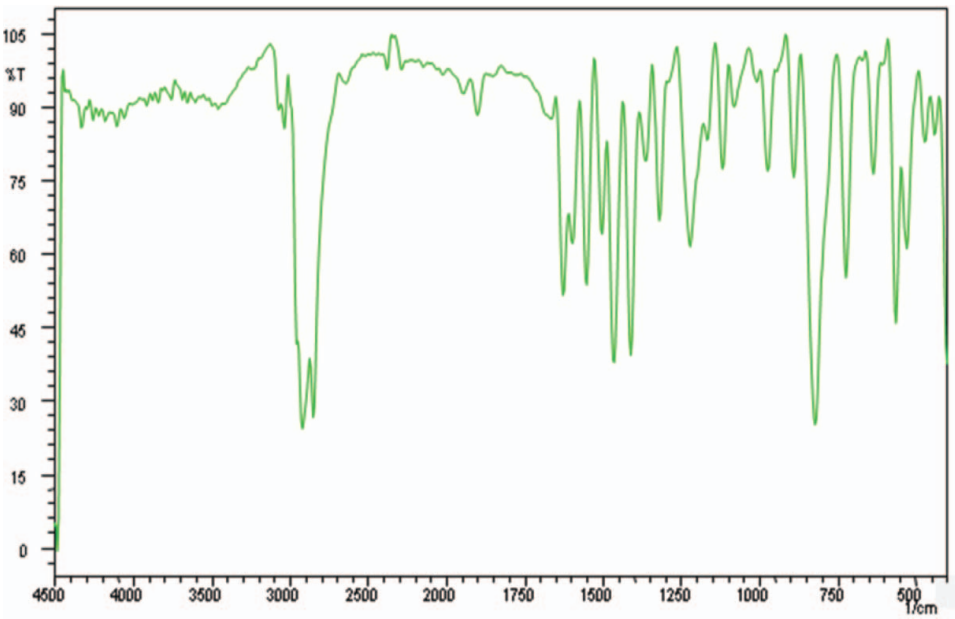

Figure 1. FTIR spectrum of Py16BA (Color figure available online).

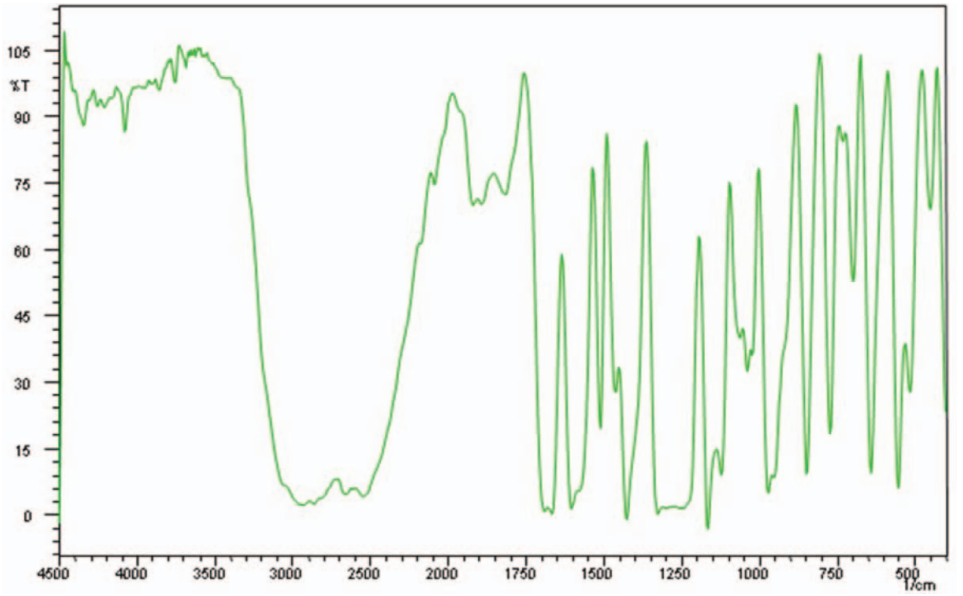

Figure 2. FTIR spectrum of 5oBA (Color figure available online).

and strong intense absorption peak in the range of 2956–2538 cm^{-1}, which implies the participation of −OH group of noBAs [16]. The observation of a double peak at 1690 cm^{-1}, characteristic of C=O stretching (of acid group), is indicative of its dimeric form. The observed peaks at 1603 cm^{-1}, 1582 cm^{-1}, and 1508 cm^{-1} are attributed to the skeletal vibrations of the aromatic system.

The FTIR spectrum of the Py16BA:5oBA complex is presented in Fig. 3 as a representation. The spectrum shows a peak in the vicinity of 3029 cm^{-1}, corresponding to the stretching mode corresponding to the C−H bond of pyridine with aromatic ring. It is also noted (in comparison with Fig. 1) that it gets shifted by 34 cm^{-1} after the formation of the HB complex. Broad peaks at 2956 cm^{-1} and 2860 cm^{-1} imply the stretching of hydroxyl −OH groups involved in hydrogen bonding [16]. A meticulous observation reveals that the C−H stretching mode of the carbonyl (aldehyde) group due to Fermi resonance is buried in it. The peak at 1685 cm^{-1} implies the C=O stretching of an acid. The peak at 1602 cm^{-1} implies the C=N stretching of the pyridine moiety. Additional peaks at 2461 cm^{-1}, 2349 cm^{-1}, and 1909 cm^{-1} imply aromatic overtones and combination bands, as they also confirm the formation of hydrogen bond between the pyridine moiety and the carboxylic acid moiety. An overview of the observed FTIR spectra and the appearance/absence of absorption lines are suggestive of the molecular structure as presented in Scheme 2.

3.2 Phase Characterization by POM

The observed phase variance and transition temperatures as determined by the textural studies with POM for the Py16BA:noBA series of HBLCs are presented in Table 2. All of the compounds are found to exhibit textures characteristic of the underlying structure [22]. For the nematic phase, a threaded marble texture is observed in the lower homologs, while higher members are found to exhibit schlieren texture. Focal conic and broken focal conic fan textures are observed for smectic-A and smectic-C phases, respectively. Transient transition

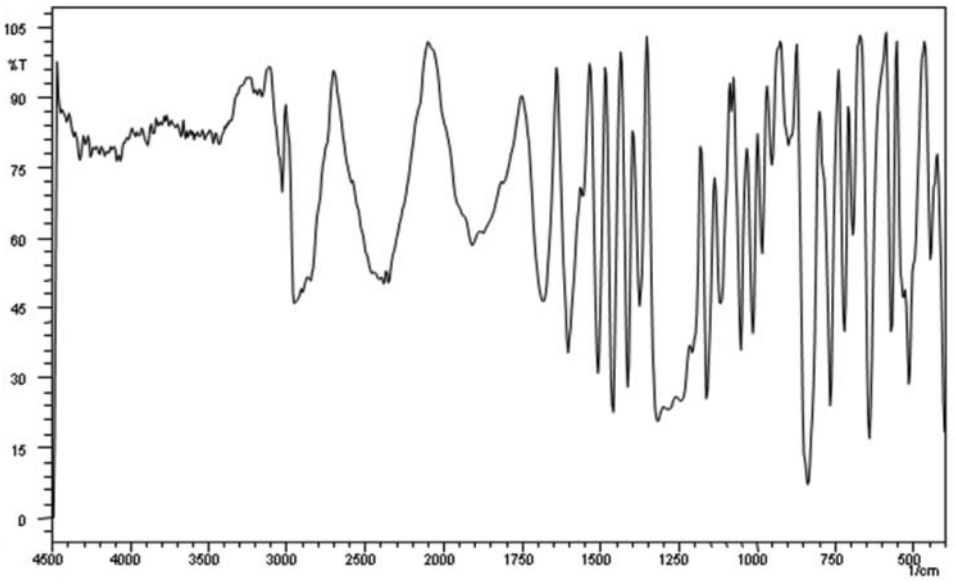

Figure 3. FTIR spectrum of Py16BA:5oBA.

bars appear (Fig. 4) across the focal conic fans in the case of compounds exhibiting smectic-A-to-smectic-B transition. The AB transition is found to be a paramorphotic change. The texture in low-temperature smectic-B phase is found to retain its appearance, except for its glossy appearance. The appearance of the transient transition bars across the focal conic fans during this paramorphotic change implies that the lower-temperature phase is crystalline smectic-B [22]. It is also noted that the occurrence of smectic-B_{cryst} is monotropic (in cooling) in nature in all the four lower homologs (i.e., $n = 3$, 4, 5, and 6) of this series. The smectic-C phase exhibited threaded marble texture. The smectic-F phase exhibited (Fig. 5) broken focal conic petal texture. A comparative study of phase abundance and thermal stability between the Py16BA:noBAs and the noBAs implies that the lower homologs of noBAs (viz., 4-propyloxy to 4-hexyloxy benzoic acids) exhibited the nematic phase in the range of about 40–50°C prevalently [4,5,9,21,23]. The lower homologs of Py16BA:noBAs do not exhibit the nematic phase. Conspicuously, the nematic phase is found to be quenched in homologs of Py16BA:noBAs. While the higher homologs of the noBA series ($n = 7$–12) are reported to exhibit both nematic and smectic-C mesophases [10,21], the intermediate and higher homologs of Py16BA:noBAs are found to exhibit tilted versions of smectic phases, i.e., smectic-C and smectic-F. However, the 1D orthogonal smectic-A and 3D orthogonal smectic-B_{cryst} (with hexagonal ordering) phases are exhibited by the lower homologs of Py16BA:noBAs. Although the presence of tilted smectic-C phase as well as its enhanced thermal stability is reported [21] in the HBLCs involving noBA moieties, the induction of a quasi- 2D smectic-F phase is found to occur from an intermediate homolog (i.e., $n \geq 7$) onward in the Py16BA:noBA series of HBLC complexes. The occurrence of smectic-F phase in the higher homologs (i.e., from intermediate homologs) with increasing chain length is found to agree with the occurrence of smectic-F phase in the higher homologs of HBLCs [10,16,21,23] and series [24–28] of LCs without hydrogen bonding. The occurrence

Table 2. Details of phase variance, transition temperatures, and enthalpy values exhibited by HBLC complexes (Py16BA:noBAs)

PyB16A: nOBAs	Method	Phase variant	Iso.– S_A/S_C	S_A/S_C– S_B/S_F	S_B/S_F– Cryst.	$[\Delta T]_{Tilt}$ in °C
Py16BA:	TM	AB	109.2	71.2	44.1	
3oBA	DSC (h)		112.7 (23.06)	[a]	85.7 (103.76)	
	DSC (c)		108.9 (21.77)	71.0 (4.56)	43.7 (105.08)	
Py16BA:	TM	AB	112.9	75.9	32.2	
4oBA	DSC (h)		118.1 (21.10)	[a]	77.4 (74.43)	
	DSC (c)		112.5 (18.49)	75.3 (4.89)	31.8 (47.51)	
Py16BA:	TM	AB	111.8	78.7	45.0	
5oBA	DSC (h)		115.1 (19.92)	[a]	86.9 (84.32)	
	DSC (c)		111.3 (19.28)	78.6 (5.86)	44.4 (83.33)	
Py16BA:	TM	AB	114.0	83.5	32.5	
6oBA	DSC (h)		118.6 (26.02)	[a]	83.3 (80.58)	
	DSC (c)		113.9 (24.09)	83.1 (7.45)	29.7 (57.20)	
Py16BA:	TM	CF	113.1	85.0	46.5	66.8
7oBA	DSC (h)		116.8 (22.37)	[a]	86.4 (79.07)	28.3[c];
	DSC (c)		112.7 (18.67)	84.4 (6.74)	45.9 (67.17)	38.5[d]
Py16bA:	TM	CF	115.9	89.1	36.5	79.6
8oBA	DSC (h)		120.2 (20.89)	92.7 ([b])	87.3 (63.12)	26.9[c];
	DSC (c)		115.5 (17.68)	88.6 (6.28)	35.9 (39.43)	52.7[d]
Py16BA:	TM	CF	114.8	85.2	34.8	80.4
9oBA	DSC (h)		119.1 (25.48)	91.4 ([b])	84.6 (74.61)	29.3[c];
	DSC (c)		114.3 (21.03)	85.0 (6.94)	33.9 ([b])	51.1[d]
Py16BA:	TM	CF	112.3	82.8	45.1	67.3
12oBA	DSC (h)		119.5 ([b])	112.5 (83.58)	91.5 (94.79)	29.3[c];
	DSC (c)		111.9 (23.65)	82.6 (9.47)	44.6 (44.4)	38.0[d]

[a]Monotropic; [b]not well resolved; [c]thermal range of smectic-C phase; [d]thermal range of smectic-F phase; values in curved braces are for enthalpy in J/g. TM-Polarized thermal microscopy (POM), h-heating, c-cooling.

of quasi-2D smectic-F phase in the higher homologs of the present Py16BA:noBAs (with long flexible end-chains) is argued [27] due to the induction of orientational disorder.

3.3 Phase-Transition Temperatures and Heat of Transitions by DSC

The phase-transition temperatures (T_c) and the enthalpy values (ΔH) observed during the differential scanning calorimetry (DSC) studies are listed in Table 2. The results of DSC are found to be in agreement with our POM studies. The phase diagram drawn for Py16BA:noBAs using the data of phase-transition temperatures (i.e., from DSC in cooling cycle) exhibited by the HBLC complexes is presented in Fig. 6. A comparison of enthalpy values across the intra-smectic phase transitions reported in HBLCs of noBAs [10,14,21] and the present Py16BA:noBAs indicate the involvement of higher values of enthalpy in the latter case. The lower enthalpy values in HBLCs of noBAs imply saturated smectic ordering among the smectic phases exhibited by the HBLCs in their dimeric form. Most

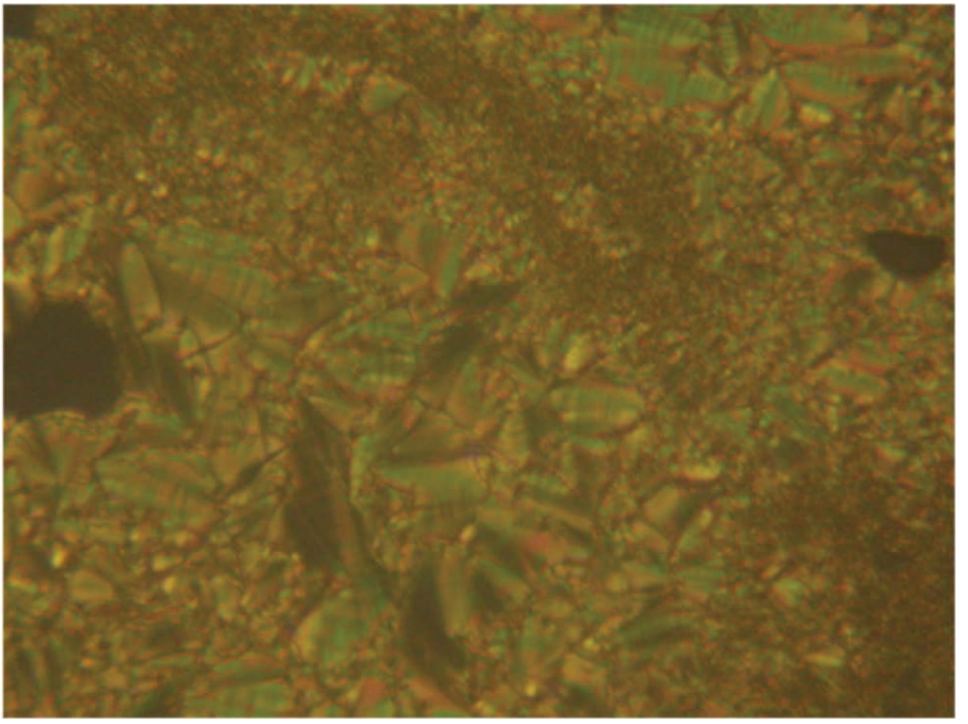

Figure 4. Transient transition bars for AB transition in Py16BA:4oBA at 75.9°C (Color figure available online).

of the compounds of Py16BA:noBA series of HBLCs are found to exhibit super-cooling, as observed in the cooling profile of DSC scans. The hydrogen bonding in noBAs is of complementary type. The electronegative O atom of the acid group acts as a proton acceptor. However, in the case of Py16BA:noBAs, the N-atom of the pyridyl derivative (which is less electronegative than the O-atom) acts as a proton acceptor. Furthermore, the hydrogen bonding in the case of Py16BA:noBAs is of linear type. Therefore, the less severe soft covalent interaction is believed to result in the observed super-cooling, leading to the occurrence of LC phases over a wide range of temperatures.

The features of distinction between the HBLCs formed exclusively of noBAs (dimers, as shown in Scheme 1) and the present case of Py16BA:noBAs are:

(a) In the former case, the flexible end-chains are present at both ends of the molecule. As the chain length is increased (by changing the n value in noBAs), the flexibility of the molecule is effected from both sides of the LC molecule. But in the latter case, the variable flexible chain is attached to one end only. It is also worthy to note that the other end has a flexible ($n = 16$ methyline [$-CH_3$] units) chain. Thus, its length is fixed. The situation of noBAs leads to the balancing (or annulling) of the possible steric and inductive effects caused by the increment in chain length, while it assumes effective in the latter case as they undergo variation from only one side of the LC molecule. Furthermore, the effect of increasing the chain length is reported to induce orientational disorder, which results

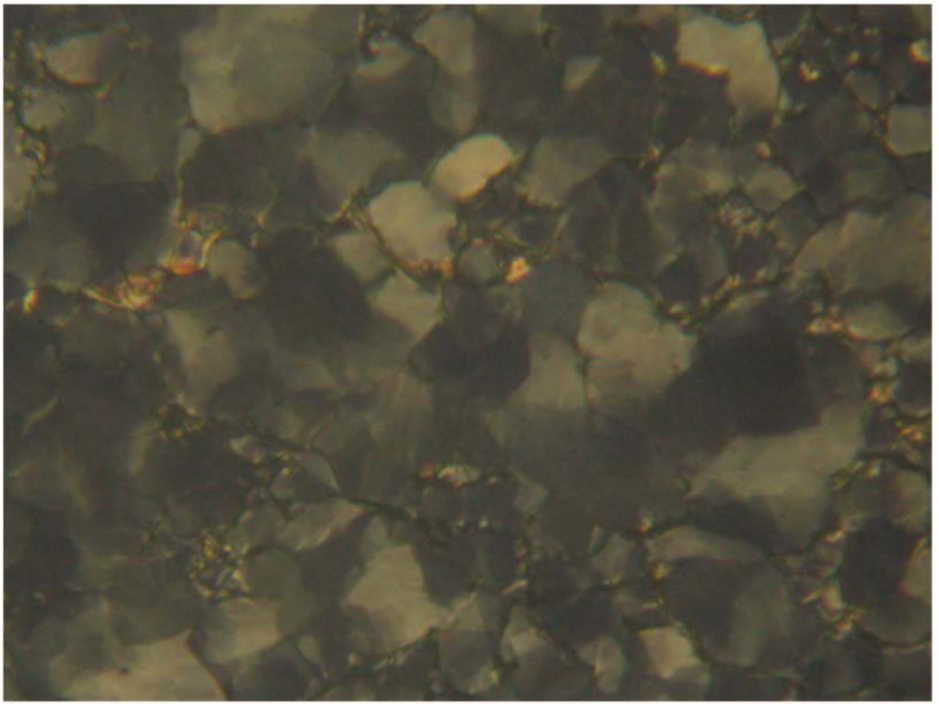

Figure 5. Broken focal conic (petal texture) of smectic-F phase in Py16BA:8oBA at 85.0°C (Color figure available online).

in the appearance of quasi-2D smectic-F phase with pseudo-hexagonal packing [27].

(b) In the former case, the essential rigid core part is made up of two aromatic moieties, while in the latter case, it consists of three aromatic moieties.

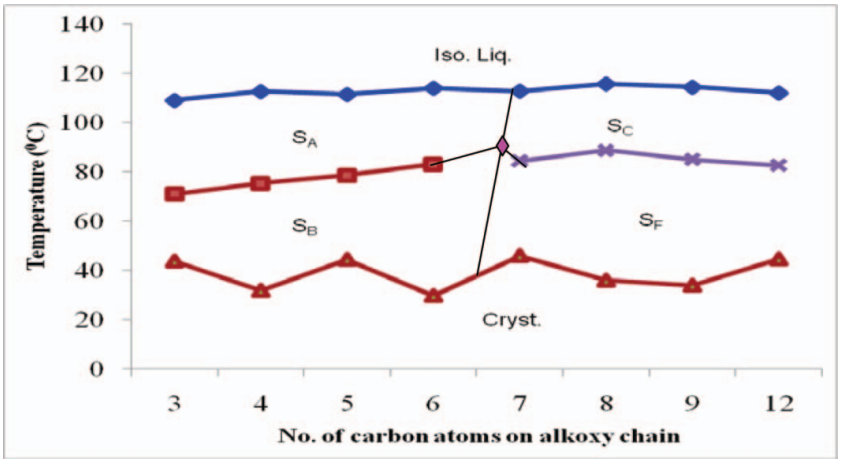

Figure 6. Phase diagram for HBLC complexes of Py16BA:noBAs (Color figure available online).

(c) In the former case of dimeric form of molecule, the complementary hydrogen bonding exists, so that the rigid core part contains higher space occupancy of soft covalent interaction, while in the latter case, it contains lesser space occupancy of soft covalent interaction (due to it being a linear hydrogen bonding type). The relatively (denser) higher space occupancy of soft covalent interaction for a dipole pair in HBLCs formed by pure noBAs leads to the comparatively destabilized conditions of a molecular dipole pair. Thus, the situation opposes the lateral stacking to form layered smectic phases.

(d) In the former case of complementary hydrogen bonding in noBAs, the proton acceptor moiety is represented by the O-atom (of the carboxylic acid moiety), while in the latter case, the N-atom of the pyridyl hexadecyl aniline serves as the proton acceptor. Although the similarity of the chemical environment regarding proton donor (H atom) is comparable (in both of the cases), the proton acceptor atoms differ (i.e., O atom in noBAs and N atom in Py16BA:nOBAs) in quality. Obviously, the electronegativity values of the proton acceptor atoms differ.

3.4 Phase Diagram for Py16BA:nOBAs

A phase diagram (Fig. 6) is drawn based on the data of phase-transition temperatures and phase abundance in Table 2. The phase diagram reflects upon the features of the odd–even effect in transition temperatures and corresponding enthalpy, the quenching of the nematic phase, induction or appearance of orthogonal and tilted (1D, quasi-2D, and 3D) smectic phases, and their stability.

An integrated view over the cited features of distinction, namely from (a) to (d) in Section 3.3, suggests the promotion of lateral stacking conditions at the cost of quenching of the nematic phase (of lower homologs) in Py16BA:noBAs. The orthogonal smectic phases that appear in the lower homologs preferentially organize as tilted smectic phases in higher (or intermediate) homologs due to the steric effects of orientational disorder (i.e., by the protrusion of a flexible chain of one layer into the adjacent layer) tuned by increasing the end-chain length.

It is also noted that the present HBLC complexes of Py16BA:noBA series are found to exhibit weak odd–even effect at the clearing transition temperatures (i.e., at IA or IC phase transitions), while the effect becomes stronger at solid (crystal) melting transition (S_B-solid or S_F-solid) phase transitions. It may be recalled that the odd–even effect is explained on the basis of the contributions of anisotropic axial polarizabilities [29–31]. It is also clear from the phase diagram that the members with an even number of carbon atoms (in the flexible end-chain) exhibit higher transition temperatures (than the corresponding odd members).

Furthermore, the complexation of noBAs with Py16BA is found to lead to the increase in the thermal range of smectic-C phase. It is worthy to note that HBLCs formed by using noBAs are reported to get induced with the smectic-G phase, which is a 3D analog of smectic-C phase [6,9–11,16,17]. However, an additional tilted quasi-2D hexagonal smectic-F phase is found to be induced in the present Py16BA:noBA series when $n = 8$. It may be recalled that smectic-F phase possesses a long-range bond orientational order along with the coexisting short-range positional order [22]. A close look into Table 1 implies that the overall thermal range of tilted polymorphism is increased due to the hydrogen bonding of noBAs with Py16BA. The present observation of enhanced tilted polymorphism in Py16BA:noBA compounds is found to agree with the other reports of HBLCs of chiral and achiral nature [10]. In the wake of fundamental [3] and applied [32] aspects of tilted

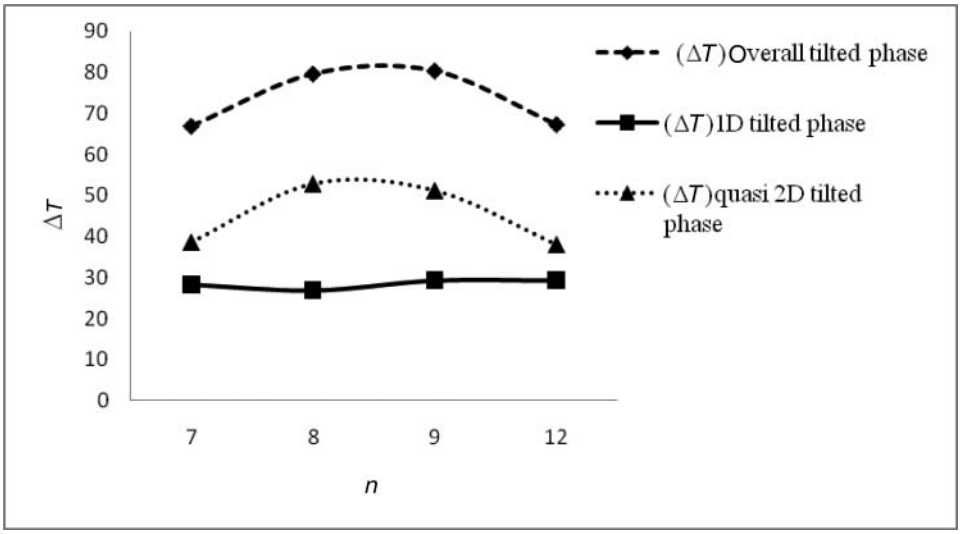

Figure 7. Variation in thermal stability of tilted LC phases with chain length (n).

smectic phases, the dependence of phase variance and thermal stability of tilted phases (viz., for overall tilted phase's thermal range, including that exhibited by smectic-C and smectic-F phases) is studied (Fig. 7) as a function of increasing chain length in the HB Py16BA:noBAs. While the overall tilted LC phase stability is found to reach its maximum at $n = 9$, the 1D tilted smectic-C phase stability exhibits saturation at $n = 9$. However, the quasi-2D tilted smectic-F phase stability reaches its maximum even at a still lower homolog ($n = 8$). It is noted that the induction of 3D tilted smectic-G phase or the increase in tilted smectic-C (or smectic-C*) phase in HBLCs is argued due to the extension (or spread) of noncovalent (soft covalent) bonding (interaction) [10], which is configured off the long axis of the LC complex. As such, the off-axis spread of interaction leads to an increase in the transverse dipole moment μ_t. It may be recalled that the enhancement in the tilted LC phase stability (smectic-C/smectic-F) in odd-numbered homologs is explained by the extension of the off-axis projection of the dipole moment in LCs [10,33]. The induction of bond orientational-ordered smectic-F phase (with pseudo-hexagonal packing in quasi-2D structure) in the higher homologs of present HBLCs is argued due to the capability of higher homologs (with longer flexible chains) to induce orientational disorder [27]. It is also noted that the induction of smectic-F phase in higher homologs of the present series agrees with the reports of induction of smectic-F phase in higher homologs of nOm series of LC compounds and other HBLCs [26].

3.5 Optimization of Tilted Smectic Phase Stability

Hydrogen bonding interaction is known to configure rather in an inclined away to the long-axis of an LC complex [10]. As such, the perpendicular drawn from the top of the outward projected vector (along the direction of soft covalent interaction) on to the long axis increases. This in turn results in the increase of μ_t. However, this increase is manifested as the observed increased thermal stability of tilted phases. The $-CH_3$ units, which are placed on the flexible end-chain part of Py16BA:noBAs, are capable of exhibiting steric protrusion (into the neighboring smectic layers) and inductive effect. However, the increasing chain

length beyond $n = 9$ (in noBA moiety) in the Py16BA:noBA series leads to a decrease in the inductive effect, while the steric intrusion (into the adjacent smectic layer) increases. The inductive effect lessens in higher homologs due to the increasing distance of end $-CH_3$ unit from the central rigid core (with soft covalent interaction). The electron-directing tendency of the $-CH_3$ unit (end-chain) on to the off-axis-inclined HB region also decreases. Thereby, the off-axis configuration of soft covalent bonding reduces. As such, its influence gets saturated with the further increase in chain length beyond $n = 9$. Furthermore, steric intrusion of the end-chain into the neighboring layers in smectic phases is found to be predominant in higher homologs. Hence, the overall (or individual) tilted smectic phase stability $[\Delta T]_{\text{Tilt}}$, i.e., $[\Delta T]_{\text{C}}$ plus $[\Delta T]_{\text{F}}$, is observed to be saturated (or optimal at $n = 9$, as in Fig. 7) with the increasing n value in Py16BA:noBA compounds.

3.6 ACBF Multi-Critical Point

A meticulous observation of the phase diagram (Fig. 6) for the Py16BA:noBA series reveals the unfailing follow-up of the odd–even effect (on T_c) along all the phase boundaries, namely AB, CF, BK, and FK (i.e., K–solid) interfaces. A logical implication of these observations when coupled with the (a) linear extrapolation of the odd–even effect at AB and BK boundaries and that at CF and FK boundaries and (b) by drawing the possible separating boundary among A, C, B, and F phases leads to the prediction of an S_A–S_C–S_F–S_B multi-critical point (MCP denoted by diamond-shaped island in Fig. 6). It is interesting to note that the orthogonal 1D smectic-A, tilted 1D smectic-C, orthogonal 3D hexagonal ordered smectic-B_{cryst}, quasi-2D tilted smectic-F with pseudo hexagonal order in LC phases with vivid geometries converge at the MCP (on the phase diagram of the Py16BA:noBA series). Thus, the synthesis of the Py16BA:noBA series of HBLCs has presented an opportunity in realizing an ACFB multi-critical point where phases underlined by relevant interesting symmetries converge.

4. Conclusions

Present investigations of HBLCs, namely the Py16BA:noBA series, through POM and DSC conclude that:

- There is a depression in clearing (smectic–isotropic liquid) transition temperatures.
- The nematic phase is quenched so as to lead to the growth of more ordered smectic phases under favorable conditions for π-bond stacking.
- Orthogonal smectic phases, namely S_A and S_B, are induced in the lower homologs due to relatively strong inductive effect.
- A quasi 2D tilted hexagonal smectic-F phase is induced in the higher homologs due to the orientational disorder introduced by the steric protrusion due to the increased chain length.
- The thermal range of tilted smectic-C phase is increased (or saturated) in the higher homologs.
- Overall LC thermal range and tilted phases' thermal ranges are increased.
- Liquid crystallinity is realized toward ambient temperatures.

Acknowledgments

D.M. Potukichi acknowledges the financial support (DST/SR/S2/CMP-0063/2008) by the Department of Science and Technology (DST), New Delhi, India. M. Srinivasulu is grateful to the Management of Manipal University for the facilities and the financial support.

References

[1] Kato, T., Fukumasa, M., & Frechet, J. M. J. (1995). *Chem. Mater.*, *7*, 368.
[2] Lehn, J. M. (1988). *Angew. Chem. Int. Ed. Engl.*, *27*, 89.
[3] de Gennes, P. G. (1993). In: Marshall & Wilkinson (Eds.), *The Physics of Liquid Crystals*, Clarendon Press: Oxford, Chapter 7, p. 277.
[4] Gray, G. W., & Jones, B. J. (1953). *J. Chem. Soc.*, 4179.
[5] Gray, G. W. (1962). *Molecular Structure and the Properties of Liquid Crystals*, Academic Press: London, p. 163 and the references therein.
[6] Paleos, C. M., & Tsiourvas, D. (1995). *Angew. Chem. Int. Ed. Engl.*, *34*, 1696.
[7] Tian, Y., Xu, X., Zhao, Y., Tang, X., & Li, T. (1997). *Liq. Cryst.*, *22*, 87.
[8] Wallage, M. J., & Imrie, C. T. (1997). *J. Mater. Chem.*, *7*(7), 1163.
[9] Srinivasulu, M., Satyanarayana, P. V. V., Kumar, P. A., & Pisipati, V. G. K. M. (2001). *Liq. Cryst.*, *28*, 1321.
[10] Sridevi, B., Chalapathi, P. V., Srinivasulu, M., Pisipati, V. G. K. M., & Potukuchi, D. M. (2004). *Liq. Cryst.*, *31*, 303; Sridevi, B., Chalapathi, P. V., Srinivasulu, M., Pisipati, V. G. K. M., & Potukuchi, D. M. (2009). *Mol. Cryst. Liq. Cryst.*, *515*, 71.
[11] Kato, T., Uryu, T., Kaneuchi, F., Jin, C., & Frechet, J. M. J. (2006). *Liq. Cryst.*, *33*, 1434.
[12] Lavigueur, E. J., Foster, E. J., & Williams, V. E. (2008). *J. Am. Chem. Soc.*, *130*(35), 11791.
[13] Dekker, A. J. (2007). *Solid State Physics*, Macmillan India: New Delhi, p. 187.
[14] Vijayakumar, V. N., & Madhu Mohan, M. L. N. (2010). *Mol. Cryst. Liq .Cryst.*, *517*, 113; Vijayakumar, V. N., & Madhu Mohan, M. L. N. (2009). *Ferrelectrics*, *392*, 1; Vijayakumar, V. N., & Madhu Mohan, M. L. N. (2010). *Physica. B*, *405*, 4418; Vijayakumar, V. N., & Madhu Mohan, M. L. N. (2009). *Solid State Commun.*, *149*, 2090; Vijayakumar, V. N., & Madhu Mohan, M. L. N. (2010). *Solid Stat. Sci.*, *12*, 482.
[15] Xiao, S., Zou, Y., Wu, J., Zhou, Y., Yi, T., Lia, F., & Huang, C. (2007). *J. Mater. Chem.*, *17*, 2483.
[16] Srinivasulu, M., Satyanarayana, P. V. V., Kumar, P. A., & Pisipati, V. G. K. M. (2001). *Z. Naturforsch*, *56a*, 685.
[17] Srinivasulu, M., Satyanarayana, P. V. V., Kumar, P. A., & Pisipati, V. G. K. M. (2001). *Mol. Mater.*, *14*, 215.
[18] Rao, N. V. S., & Pisipati, V. G. K. M. (1983). *Phase Trans.*, *3*, 317.
[19] Kohlmeier, A., & Janietz, D. (2007). *Liq. Cryst.*, *34*, 65.
[20] Silverstein, R. M., Bassler, C. G., & Morrill, T. C. (1981). *Spectroscopic Identification of Organic Compounds*, 4th ed., John Wiley: New York.
[21] Sidertou, Z., Tsiourvas, D., Paleos, C. M., & Skoulios, A. (1997). *Liq. Cryst.*, *22*, 51.
[22] Gray, G. W., & Goodby, J. W. (1984). *Smectic Liquid Crystals – Textures and Structures*, Leonard Hill: London.
[23] Kato, T., Fukumasa, M., & Frechet, J. M. J. (1995). *Chem. Mater.*, *7*, 368.
[24] Alapati, P. R., Potukuchi, D. M., Rao, N. V. S., & Pisipati, V. G. K. M. (1988). *Liq. Cryst.*, *3*, 1461.
[25] Srinivasulu, M., Potukuchi, D. M., & Pisipati, V. G. K. M. (1997). *Z. Naturforsch.*, *52a*, 713.
[26] Pisipati, V. G. K. M. (2003). *Z. Naturforsch.*, *58a*, 661.
[27] Padmaja, S., Rao, M. R. N., Datta Prasad, P. V., & Pisipati, V. G. K. M. (2005). *Z. Naturforsch.*, *60a*, 296.

[28] Pisipati, V. G. K. M., George, A. K., Srinivasu, Ch., & Murty, P. N. (2003). *Z. Naturforsch.*, *58a*, 103.
[29] Marcelja, P. (1974). *J. Chem. Physics.*, *60*, 3599.
[30] Van Hecke, G. R., Santarsiero, B. D., & Theodore, L. J. (1978). *Mol. Cryst. Liq. Cryst.*, *45*, 1.
[31] Takanishi, M., Mita, S., & Kondo, S. (1987). *Phase Trans.*, *9*, 1; Takanishi, M., Mita, S., & Kondo, S. (1987). *Mol. Cryst. Liq. Cryst.*, *147*, 99.
[32] Goodby, J. W., Blinc, R., Clark, N. A., Lagerwall, S. T., Osipov, S. A., Pikin, S. A.,Sakurai, T., Yushinao, Y., & Zeks, B. (1991). In: G. W. Taylor (Ed.), *Ferroelectric Liquid Crystals, Principles, Properties and Applications*, Chapter VI, Gordon & Breach: Philadelphia, PA.
[33] Padmaja, S., Srinivasulu, M., & Pisipati, V. G. K. M. (2003). *Z. Naturforsch.*, *58a*, 573.